OFFICE OF NAVAL RESEARCH

Contract N00014-85-K-0805, Mod/Amend P00001

Technical Report No. 1

Applications of Scanning Tunneling Microscopy to Electrochemistry

by

Moris M. Dovek, Michael J. Heben, Nathan S. Lewis, Reginald M. Penner, and Calvin F Quate

Prepared for Publication as a Chapter in an ACS Symposia Series Volume (ed. by M. P. Soriaga)

Molecular Phenomena at Electrode Surfaces

California Institute of Technology
Department of Chemistry
Pasadena, California 91125

October 28, 1988

SECURITY CLASSIFICATION OF THIS PAGE

REPORT DOCUMENTATION PAGE

1a REPORT SECURITY CLASSIFICATION Unclassified	1b RESTRICTIVE MARKINGS
2a SECURITY CLASSIFICATION AUTHORITY	3 DISTRIBUTION / AVAILABILITY OF REPORT Approved for Public Release and Sale Distribution Unlimited
2b DECLASSIFICATION / DOWNGRADING SCHEDULE	
4 PERFORMING ORGANIZATION REPORT NUMBER(S) ONR Technical Report #1	5 MONITORING ORGANIZATION REPORT NUMBER(S)
6a NAME OF PERFORMING ORGANIZATION Nathan S, Lewis Caltech 6b OFFICE SYMBOL (If applicable)	7a NAME OF MONITORING ORGANIZATION
6c ADDRESS (City, State, and ZIP Code) M.S. 127-72 California Institute of Technology Pasadena, CA 91125	7b ADDRESS (City, State, and ZIP Code)
8a NAME OF FUNDING / SPONSORING ORGANIZATION Office of Naval Research 8b OFFICE SYMBOL (If applicable)	9 PROCUREMENT INSTRUMENT IDENTIFICATION NUMBER N00014-85-K-0805, Mod/Amend: P00001
8c ADDRESS (City, State, and ZIP Code) Attn. Code 413 800 N. Quincy St Arlington, VA 22217	10 SOURCE OF FUNDING NUMBERS PROGRAM ELEMENT NO. / PROJECT NO. / TASK NO. / WORK UNIT ACCESSION NO

11 TITLE (Include Security Classification)

Applications of Scanning Tunneling Microscopy to Electrochmistry

12 PERSONAL AUTHOR(S)
Dovek, M.M., Heben, M.J., Lewis, N.S., Penner, R.M. and Quate, C.F.

13a TYPE OF REPORT	13b TIME COVERED	14 DATE OF REPORT (Year, Month, Day)	15 PAGE COUNT
Technical	FROM Sept 87 TO Aug 88	1988, Oct 28	29

16 SUPPLEMENTARY NOTATION

17 COSATI CODES		
FIELD	GROUP	SUB-GROUP

18 SUBJECT TERMS (Continue on reverse if necessary and identify by block number)
Review, STM, Electrochemistry. (mgm) €

19 ABSTRACT (Continue on reverse if necessary and identify by block number)

The Scanning Tunneling Microscope has demonstrated unique capabilities for the examination of electrode topography, the vibrational spectroscopic imaging of surface adsorbed species, and the high resolution electrochemical modification of conductive surfaces. Here we discuss recent progress in electrochemical STM. Included are a comparison of STM with other *ex situ* and *in situ* surface analytic techniques, a discussion of relevant STM design considerations, and a semi-quantitative examination of faradaic current contributions for STM at solution-covered surfaces. Applications of STM to the *ex situ* and *in situ* study of electrode surfaces are presented.

20 DISTRIBUTION / AVAILABILITY OF ABSTRACT ☒ UNCLASSIFIED/UNLIMITED ☐ SAME AS RPT ☐ DTIC USERS	21 ABSTRACT SECURITY CLASSIFICATION Unclassified
22a NAME OF RESPONSIBLE INDIVIDUAL	22b TELEPHONE (Include Area Code) / 22c OFFICE SYMBOL

DD FORM 1473, 84 MAR 83 APR edition may be used until exhausted
All other editions are obsolete

SECURITY CLASSIFICATION OF THIS PAGE

Applications of Scanning Tunneling Microscopy to Electrochemistry

Moris M. Dovek[1], Michael J. Heben[2], Nathan S. Lewis[2*], Reginald M. Penner[2], and Calvin F. Quate[1*]

[1]Department of Applied Physics, Stanford University, Stanford, CA 94305
[2]Department of Chemistry, Stanford University, Stanford, CA 94305
*Address correspondence to these authors.

The Scanning Tunneling Microscope has demonstrated unique capabilities for the examination of electrode topography, the vibrational spectroscopic imaging of surface adsorbed species, and the high resolution electrochemical modification of conductive surfaces. Here we discuss recent progress in electrochemical STM. Included are a comparison of STM with other *ex situ* and *in situ* surface analytic techniques, a discussion of relevant STM design considerations, and a semi-quantitative examination of faradaic current contributions for STM at solution-covered surfaces. Applications of STM to the *ex situ* and *in situ* study of electrode surfaces are presented.

Since its introduction by Binnig *et. al.* in 1982 (1,2), the scanning tunneling microscope has proven to be a powerful and unique tool in the study of surfaces. The technique is conceptually simple but technologically demanding: a conducting filament of 1-10 Å width at its point is placed within several angstroms of a conducting surface, and the tunneling current is monitored while the tip is rastered across the sample surface. Surface structure has been obtained with atomic resolution in a variety of ambients, including ultra-high vacuum (3-8), cryogenic fluids (9-10), atmospheric pressure of air (11-14), and liquid solutions (*vide infra*). Additionally, electronic information about surfaces (15-18), and vibrational information about surface adsorbates (10) has been obtained on atomic dimensions. Several review articles that describe in depth the accomplishments and promise of STM have been published (19-23). Clearly, these advances in surface characterization have the potential to impact electrochemistry in diverse areas, including small scale lithography, *in situ* characterization of electrodes and of double layer structure, spectroscopy of adsorbed intermediates, and electronic properties of electrode materials.

To date, most STM studies have focused on demonstrating the breadth of the possible applications; consequently, there are relatively few studies of a single electrode/electrolyte interface as compared to, for example, surface enhanced Raman spectroscopy on the Ag/pyridine system (24-26). Application of STM to electrochemistry will require modification of current microscope designs, and will present challenges in the integration of electrochemical potential control as well as in techniques for data collection and workup. In this paper, we attempt to review the progress made in this relatively young field, and attempt to develop some of the theory and applications germane to use of the STM in an electrochemical environment. We first compare STM with other *ex situ* and *in situ* electrode surface characterization techniques. We then discuss modifications in microscope design that are necessary for use in electrochemical cells, and proceed to develop a semiquantitative discussion of the theory of STM imaging in an electrochemical environment. We then will review the uses of STM as an *ex situ* tool for the characterization of electrochemical surfaces, and finally will discuss experiments that have taken advantage of the STM for *in situ* characterization and modification of electrode interfaces.

Comparison of Scanning Tunneling Microscopy with Other Surface Characterization Methods

At present, the STM has been demonstrated to yield spectroscopic information regarding the spatial, vibrational, and electronic structure of surfaces. In all of these areas, the STM is complementary to other existing techniques. Also, and in many potential applications, STM possesses unique features and capabilities. These capabilities are discussed in the section below.

Structural Information. To a first approximation, the structural information from an STM image results from variations in the electronic wavefunctions of a surface due to the positions of the surface atoms (20,27,28). Structural information can be obtained by rastering across the surface of interest while employing negative feedback to maintain a constant tunneling current. By monitoring the movement of the tip relative to the surface an image can be obtained (2,29). If the time constant of the feedback loop is increased so that a constant height, rather than a constant current is maintained, then the spatial variation of the tunneling current will contain structural information (30). Manipulation of the tip on an angstrom level is accomplished by use of piezoelectric materials, and further details regarding this process can be found in the section on microscope design.

In STM, the localized nature of the tip-surface interaction results in an inherently sensitive probe of surface topography. Resolution in the direction perpendicular to the surface (the z-direction) can be as high as 0.1 Å (31), while resolution in the lateral direction can approach < 2 Å (20,32). The image frame area varies somewhat, depending upon the details of the microscope, but typically lies in the range of 1 μm. Due to the necessity of producing a tunneling current, STM experiments generally require a

conducting or semiconducting surface, although the related atomic force microscope (AFM) can yield similar topographical information on insulating surfaces (33-35).

As an *ex situ* technique for structural information on surfaces, STM is an excellent complement to the standard electron and ion diffraction probes of surface order. The STM method can identify both short range order and long range periodicity, as well as disordered surface layers (*e.g.*, images of sorbic acid on Highly Ordered Pyrolitic Graphite (HOPG), *vida infra*). In contrast, LEED requires a coherence length of ordered domains on the order of at least 100 Å to be useful (36). SEM images are typically limited to resolution of 50 Å, but are useful due to their depth of field and wide field of view (37). High resolution TEM can yield images of solids to a resolution of 1-2 Å, but requires extensive sample preparation and also requires that the surface atoms be in registry with the remainder of the bulk sample under study (14,38). Clearly, each technique provides valuable information which complements the others, and ideally a combination of the probes would be used to obtain a complete characterization of the surface under study.

For *in situ* surface studies under modest pressures of ambient gases, or for *in situ* studies of surfaces in contact with liquids, the ion and electron diffraction techniques are not available. In these systems, STM becomes one of the few techniques capable of yielding surface topographic information. Under certain conditions, surface EXAFS and X-ray standing wave techniques can yield information concerning the periodicity and lattice properties of a surface layer (39-41), however, these techniques yield average values of the desired signal over macroscopically large (mm^2) beam areas (39-41). Ellipsometry can yield information concerning the morphology of surface layers provided that suitable models for the interface have been developed and confirmed by complementary techniques (42,43). Clearly, the overall lack of *in situ* structural probes of surfaces is a major driving force behind application of STM to electrochemical interfaces.

Vibrational and Electronic Spectroscopy. STM has recently been applied as a surface vibrational spectroscopic tool. To date, the applications have been for surfaces prepared under ambients, and examined subsequently *ex situ*. For example, Smith *et. al.* (10) have obtained vibrational information from adsorbed sorbic acid molecules on highly ordered pyrolytic graphite substrates. In this application, STM competes most closely with EELS (44), IETS (45), FTIR (46) and Raman spectroscopy (47). Each probe has particular advantages with respect to spectral range, resolution and the types of systems that may be studied. The selection rules that apply to vibrational spectroscopy with the STM have not yet been elucidated. If the interaction is dipolar in nature, then it might be expected that there must be some component of the vibrational mode's electric dipole moment which is parallel to the exciting tunneling beam in order to obtain a signal. A potential advantage of the STM technique is that molecular vibrational modes may be probed on an individual molecule-by-molecule basis (10). Although the limits of applicability of STM to vibrational spectroscopy have only recently begun to be explored, a distinguishing feature is the inherently

small "effective beam size" of the technique and possible geometric information afforded by the vibrational spectra (10).

STM has also been shown to provide surface electronic information (1). The most common application to date in this area is use of STM to probe the density of states in metals and semiconductors. Materials of interest to electrochemists that have been investigated include Si (17,48), GaAs (16,49), graphite (18), Pd (15), and Au (15). Once again, STM's unique contribution in these applications arises from the small areas (ca. 2-4 $Å^2$) that are involved in the measurement process. These capabilities have enabled the mapping of the spatial distribution of electronic states. For example, cation and anion sites on GaAs surfaces have been discriminated (Stroscio, J.A.; Feenstra, R.M.; Newns, D.M.; Fein, A.P. J. Vac. Sci. Technol. A, in press)(3). Electronic structure measurements of occupied states are typically made with UPS, while unoccupied states are probed by IPS (49). EELS probes both filled and unfilled states simultaneously, and is therefore used in conjunction with either UPS or IPS to complete a band structure determination (44,49). A new electronic spectroscopy technique, Field Emission Scanning Auger Microscopy (50), utilizes STM-like technology to effect highly localized (c.a. 1 μm) Auger electron spectroscopy. The local electronic information afforded by STM is a valuable complement to these other techniques, and STM is the only one of these methods that may be applied to *in situ* investigations in condensed media.

Microscope Design for Electrochemical Applications

The critical aspects of STM design deal with the formidable task of separating detected spatial variations of electronic wavefunctions, and signals derived therein, from spurious mechanical, acoustical, and thermally derived noise (51). Stated in another way: the task is to isolate and control the vertical and lateral confines of an electron tunneling current. Important developments facilitating this goal include the introduction of magnetic levitation (1), eddy current damping (2,21), and spring supported staging (21,30) for vibration isolation. Simplicity of design was gained through the realization that stacked plates separated by lossy elastomers could achieve similar ends (52,53). High speed imaging techniques, employable on relatively smooth surfaces, were found to yield an improved signal-to-noise ratio (51,54) and, consequently, opened the real time imaging domain. The invention of the piezo tube scanner by Binnig and Smith (56) further reduced the complexity of microscopes and, since mechanical resonances of the tube occur at higher frequencies (c.a. 8 kHz), the tube scanner allows still higher tip speeds. Throughout these design evolutions the need for compactness and rigidity in the microscope body has been respected (55).

The design criteria for an *in situ* electrochemical STM include the above outlined considerations as well as several needs peculiar to an electrochemical environment. Sonnenfeld and Hansma (57) constructed the first STM to operate under solution. Their work highlights two important design considerations. Firstly, the tip and sample should be the only electrically active parts of the microscope exposed to solution. This first solution microscope was

designed such that the piezoelectric scanning elements could remain above the solution level. In taking this design consideration further, we suggest that the tip and sample should be the only chemically reactive parts (*e.g.*, metal) of the microscope exposed to solution.

The importance of tip insulation is the second significant solution microscope design feature recognized by Sonnenfeld and Hansma (57). Except in ideally pure solutions faradaic currents will always be present between the tip and sample. If these currents are of the same magnitude as the tunneling currents, then feedback control will be difficult to maintain. Commercially available Pt-Ir tips, which are glass coated except for about 50 μm at the tip end, were employed in an effort to reduce faradaic currents. The most recent efforts by Sonnenfeld *et. al.* involved the use of Pt-Ir tips with all but 5 μm insulated from the electrolyte (58). SiO was then deposited on the uninsulated section of the tip by evaporation, and this dielectric was subsequently removed from the very end of the tip by approaching into tunneling range with a 10 V bias between the tip and sample (Schneir, J.; Hansma, P.K.; Elings, V.; Gurley, J.; Wickramasinghe, K.; Sonnenfeld, R. SPIE'88 Conference Proceedings, in press). Such tips have also been employed in a newer STM, shown in Figure 1, that employs a single tube scanner, and allows for fluid delivery and removal via a fluid transfer line. This approach, discussed in greater detail below, was successful in that Au could be plated from, and imaged with, these tips (58).

Other workers who have reported STM under solution include Itaya *et. al.* (59) and Fan *et. al.* (Fan, F-R.F.; Bard, A.J. Anal. Chem., submitted). Their instruments each employ three orthogonal piezoelectric elements as tip translators and both use glass tip insulation, though their tip preparation techniques differ. In the former case, a 10 μm Pt wire was sealed into a capillary and subsequently etched, while the latter workers used a 65 μm Pt wire which was sealed in soft glass, turned on a lathe, and then sonicated in concentrated H_2SO_4.

Morita and co-workers (60) have constructed a STM that employs a unique 3D scanner and 3D positioner that is constructed from several piezoelectric cubes. This microscope was subsequently equipped with an electrochemical cell that allows disconnection of the tip and conventional 3 electrode voltammetry to be performed (61). Itaya *et. al.* have gained similar capabilities by modifying their aforementioned STM (Itaya, K.; Higaki, K.; Sugawara, S. Chem. Lett., in press).

A noteworthy advance in the design of solution STMs was achieved by Lev *et. al.* (Lev, O.; Fan, F-R.F.; Bard, A.J. J. Electroanal. Chem., submitted) by including a Pt "flag" electrode in the STM of Fan *et. al.* (Fan, F-R.F.; Bard, A.J. Anal. Chem., submitted). A battery between the sample and this flag electrode, which remains poised at the rest potential of the solution, enables the sample to be biased away from the rest potential independently of the tip to sample bias.

We have also recently constructed a STM suitable for work under solution (see Fig. 2). The salient features of our design include the fact that only tip, sample, pyrex, and teflon are exposed to solution. An automatic approach mechanism allows for the

remote operation of the microscope in an N_2 drybox and facilitates the preparation of glass coated tips via a field emmision process that is similar to Sonnenfeld's. The microscope can be operated with a reference electrode, counter electrode, and bi-potentiostat to provide the above mentioned capabilities used by Lev and co-workers. A more complete discussion of this microscope design can be found elsewhere (Dovek, M.M.; Heben, M.J.; Lang, C.A.; Lewis, N.S.; Quate, C.F. Rev. Sci. Instr., submitted).

Currents in an Electrochemical STM Experiment

The key behind the imaging capabilities of the STM is the ability to control and monitor the tunneling current between the tip and the sample. To a first approximation, the tunneling current is related to the interelectrode spacing, d, by the expression (1,30):

$$i_t \propto \Delta E_t \exp(-2\kappa d) \qquad [1]$$

where κ is the decay constant for the wave function in the tunneling barrier, and ΔE_t is the tunneling bias. For a typical value of κ = 1.0 $Å^{-1}$ and a constant bias, equation [1] predicts a decrease in the tunneling current of an order of magnitude with a 1 Å decrease in the tip-substrate distance. Thus, equation [1] requires that tip-sample spacings of less than 10 Å be employed for imaging at moderate biases (ΔE_t < 1 V) in STM (20).

In any imaging and spectroscopic mode of the STM, a bias is required between the sample and the tip. In an electrochemical solvent, faradaic current between the tip and sample can interfere with, and sometimes completely obscure, the tunneling current. This undesirable situation makes it very difficult to control the feedback and to maintain a constant tunneling gap between the tip and the sample. For example, in our laboratory, we have found that feedback control is lost on our present microscope if the faradaic current, i_F, assumes a value greater than one-half that of the tunneling current, i_t. Use of partially insulated tips alleviates this condition, but unfortunately, does not completely eliminate the problem (57).

For the operation of an STM in a conventional two-electrode configuration, the presence or absence of significant faradaic current in the tip-sample circuit depends on three factors: 1) the redox potential(s) of the solution species, 2) the reversibility of the electron transfer events for the dissolved redox couple(s), and, 3) the extent to which solution species are permitted access to the tunneling gap. We have identified four limiting cases of electrochemical interest, and discuss each separately below.

Case I: Pure Liquids and Inert Electrolytes. In the absence of significant impurity currents, no faradaic current will flow if the applied bias between the tip and substrate, ΔE_t, is less than the total potential difference, $\Delta E_{F,rev}$, required to drive faradaic reactions at the STM tip and at the substrate. This condition can be easily calculated from the electrochemical potential data for the solvent/electrolyte system under study. This situation is most likely to exist in pure liquids or in solutions of nonelectroactive electrolytes where the faradaic reactions at both electrodes are

associated with solvent or electrolyte electrolysis. The bias window available for imaging under these circumstances can be 1 V or more. In pure water at room temperature, for example, $\Delta E_{F,rev} = 1.2$ V (62). In such cases, it may be unnecessary to employ insulated STM tips. From a practical standpoint, however, such tips are desirable since the magnitude of the residual (impurity) faradaic current present at any tunneling bias is reduced.

Case II: Reversible or Quasi-Reversible Redox Species. If the tip-sample bias is sufficient to cause the electrolysis of solution species to occur, *i.e.*, $\Delta E_t > \Delta E_{F,rev}$, the proximity of the STM tip to the substrate surface ($d < 10$ Å) implies that the behavior of an insulated STM tip-substrate system may mimic that of a two-electrode thin-layer cell (TLC)(63). At the small interelectrode distances required for tunneling, a steady-state concentration gradient with respect to the oxidized (Ox) and and reduced (Red) electroactive species should be established between the tip and the substrate, and the resulting steady-state current will augment that present as a result of the convection of electroactive species from the bulk solution. In many cases, this steady state current is predicted to overwhelm the convective currents, so this situation is of concern when STM imaging under electrochemical conditions (64).

Davis *et. al.* (64) have calculated the steady-state thin-layer current component for a series of electrode geometries. In their derivation, these authors have assumed that the flux between the electrodes is one-dimensional (perpendicular to the plane). Particularly relevant to the STM geometry are the equations for the current in a conical electrode/planar electrode TLC, I_{con}, and those for a hemispherical electrode/planar electrode TLC, I_{hsph} (64):

$$I_{con} = (1 + \alpha^2)^{1/2}(0.5 - \gamma/4 \ln (1 + 2/\gamma)) \qquad [2]$$

$$I_{hsph} = \ln (1 + \gamma\text{-}1) \qquad [3]$$

In the above equations, α is the conical aspect ratio, r/h; γ is the ratio of the cone or hemisphere radius to the interelectrode distance, r/d; and I, the dimensionless faradaic current (either I_{con} or I_{hsph}), is the ratio between the one-dimensional current contribution, i_{TLC}, and the limiting current for an isolated hemispherical electrode, i_{hsph} (see Eq. 5)(64):

$$I = \frac{i_{TLC}}{i_{hsph}} \qquad [4]$$

A plot of I for both conical and hemispherical geometries is shown in Figure 3. The thin-layer current component for these two geometries becomes significant for interelectrode distances on the order of the cone/hemisphere radius; *i.e.*, that of the steady state diffusion layer thickness for microelectrodes with these geometries. At smaller distances, $d < r$, the values of I for these two cases diverge. The value of I for the hemisphere/plane system approaches infinity at small r, in analogy to twin planar electrode TLC's. In contrast the cone/plane TLC reaches a limiting value (64) at small interelectrode separations. Digital simulations performed by the

authors indicate that lateral (non-one-dimensional) diffusion can be expected to contribute less than 10% of the total current for the hemisphere/plane case and for an interelectrode distance, $d < 0.01\ r$ (64). It should be noted that the accuracy of Equations 2 & 3 has not yet been demonstrated experimentally.

Equations 3 & 4 permit the faradaic current to be estimated for a hemispherical tip geometry and small values of γ; *i.e.*, at the limit of small interelectrode distances. At a typical tunneling distance of 10 Å, assuming the tip radius, $r = 1\ \mu m$ ($\gamma = 10^{-3}$), and $D = 10^{-5}\ cm^2\ sec^{-1}$, the concentration of electroactive species corresponding to $i_{TLC} = 1$ nA is 0.24 μM. At the limit of large interelectrode spacings, (*i.e.*, $\gamma >> 1$) the steady-state diffusion-layer thickness $r_{ss} < d$, and Figure 3 shows that the one-dimensional TLC current, i_{TLC}, component will be small. Assuming the current, i_{hsph}, under these circumstances is limited by diffusion to a hemispherical microelectrode at the STM tip, its magnitude will be given by (65):

$$i_{hsph} = 2\pi nFRDC_{ox/red} \qquad [5]$$

Thus, for $R = 1\ \mu m$ and $D = 10^{-5}\ cm^2\ sec^{-1}$, a 1 nA limiting current is obtained for concentrations of electroactive species, $C_{ox/red} = 1.6\ \mu M$. These calculations suggest that in the presence of a reversible redox couple at micro-molar concentrations, even STM tip-sample biases of $\Delta E_t < 10$ mV will drive a faradaic current that is comparable to that of the tip-sample tunneling current. STM imaging under such circumstances is likely to be experimentally demanding using conventional feedback methodology.

This constraint may be relaxed somewhat for quasi-reversible redox couples. In this case, a significant overpotential, η, ($\eta = E - E_{rev}$), may be associated with the generation of faradaic current at one or both electrodes. Thus, it may be possible to exceed the faradaic potential window ($\Delta E_t > \Delta E_{rev}$) without drawing significant faradaic current due to the fact that reactions at one or both electrodes are kinetically slow. In this case, the effective faradaic potential window is given by, $\Delta E_F = \eta_a + \eta_c + \Delta E_{rev}$ ($i_F < 0.5\ i_t$). At smaller biases, feedback control can be maintained, and STM imaging ought to be possible. This case, however, has not as yet been demonstrated and all STM images of solution covered surfaces to date have been obtained with biases conforming to Case I conditions.

It should be noted here that the ultra thin-layer cells (UTLC) which result from the close approach of an STM tip to a conducting substrate may have important electroanalytical applications in studies other than STM imaging (64). This is because extremely large current densities should be attainable in such cells, and also because of the fast transit times (*e.g.*, 50 nsec for d = 10 nm) for reactants across the cell. Thus, such UTLC's might facilitate the determination of fast heterogeneous rate constants or the study of reactive electrochemical intermediates (64).

Case III: Irreversible Electron Transfer or Insoluble Products. Steady-state currents due to one-dimensional flux between the STM tip and substrate will not exist if either, 1) the products at both electrodes are insoluble, or, 2) the electron transfer reactions at

both electrodes are irreversible. In both of these cases, the flux to both electrodes will only be that supplied from bulk diffusion into the gap.

Although from a diffusional standpoint, these two cases are indistinguishable, it should be noted that STM imaging during the deposition of insoluble products on either the substrate or tip is likely to be experimentally challenging. The accumulation of more than ca. 10 Å of nonelectronically conductive material on the substrate or tip, for example, will prevent the feedback from establishing the distances required for tunneling. Depositions of conductive materials on the STM tip (*e.g.*, metals) will probably result in detrimental changes in its geometry which reduce resolution. One experimentally accessible case may prove to be the deposition of electronically conductive materials on the substrate, *e.g.*, metal plating. In this case, control of the tunneling current is possible providing the deposition rate does not exceed the response time of the feedback circuit.

If the total current can be assumed to be limited by diffusion to the STM tip, Case III is similar to diffusion to a microdisk electrode (one electrode) thin-layer cell (63). Murray and coworkers (66) have shown that for long electrolysis times, diffusion to a planar microdisk electrode TLC can be treated as purely cylindrical diffusion, provided that the layer thickness is much smaller than the disk diameter (66). In contrast to the reversible case discussed above (Case I), the currents in this scenario should decrease gradually with time at a rate that is dependent on the tip radius and the thickness of the interelectrode gap. Thus, for sufficiently narrow tip/sample spacings, diffusion may be constrained sufficiently (i_T decayed) at long electrolysis times to permit the imaging of surfaces with STM.

Case IV: Spatial Exclusion From the Tunneling Gap. Throughout the discussion of diffusion above, we have assumed that the STM tip behaves as a microelectrode, *i.e.*, possesses a small metal area that is exposed to solution. This is typically the case with commercially available, glass insulated STM tips where the exposed metal surface area is typically 10 - 50 μm^2 (57,58). Moreover, the discussion has also assumed that diffusional processes between the STM tip and substrate are unperturbed by steric effects due to the presence of the narrow gap which separates these electrodes during tunneling. However, at typical tunneling distances, $d < 10$ Å, it is conceivable that electroactive species will be squeezed out of the tip-sample region and precluded from reacting at either the STM tip or the substrate. Alternatively, it may be possible to prepare insulated STM tips with geometries which prevent electroactive species from interacting with exposed metal at the tip. We have preliminary experimental results (*vide infra*) which suggest that these conditions can be met in practical STM tips. Thus, the spatial exclusion of electroactive species from the tunneling gap is considered here to be a fourth distinct classification for the imaging of solution-covered surfaces.

Ex Situ Electrochemical Applications of STM

Predictably, the first STM studies of electrode surfaces were *ex-situ* investigations of electrodes that were prepared in solution and subsequently imaged either *in vacuo* or in air. Several representative examples, illustrating the uses of STM to date, are discussed in this section.

Electrode Surface Topography. STM images of electrochemically pretreated platinum surfaces were first obtained in UHV by Baro and coworkers (67). The images reported by these workers were the first structural images of electrode surfaces that had been exposed to solution under potential control. In an initial series of experiments, Pt(111) single crystal electrodes were subjected to a large amplitude, square-wave potential perturbation (1M H_2SO_4, E_1 = 1.4 V, E_2 = 0.05 V vs. NHE, f = 2.5 kHz), and were imaged (at nanometer resolution) before and after the electrochemical treatment. The cyclic voltammograms in the H adsorption region, recorded as a function of time after the application of the square wave program, revealed an increase in the amount of "strongly" adsorbed H (E = 0.28 V)) as compared to "weakly" adsorbed H (E = 0.12V). This was consistent with the development of micro-crystalline regions of Pt(100) on the Pt(111) surface (67). STM images of the electrochemically treated surfaces revealed the development of atomically smooth facets on some regions of the surface, which was consistent with the proposed development of Pt(100) micro-crystallites. On the basis of both STM and electrochemical examination of Pt surfaces that were initially either polycrystalline Pt or Pt(111) oriented crystals, the authors concluded that preferential development of Pt(100) microcrystallites occurs with application of the square-wave, electrochemical perturbation (67).

Subsequent STM examinations of electrochemically pretreated platinum surfaces in air by Baro and coworkers (68) and by Fan and Bard (Fan, F-R.F.; Bard, A.J. Anal. Chem., submitted) have focused on identifying changes in the surface topography effected by electrochemical activation. In related experiments, Fan and Bard have imaged Pt single crystals and annealed polycrystalline Pt surfaces at nanometer resolution before and after the exposure of these surfaces to adsorbates such as I_2 and ethyl acetate. Images of the adsorbate-covered surfaces exhibited a qualitatively rougher topography as compared to clean Pt surfaces. However, the resolution in these images was insufficient to permit identification of these surface features.

Morita *et. al.* (69) have obtained STM images of electrically insulating, electrochemically generated, Al_2O_3 barrier layers. The Al_2O_3 surfaces to be imaged were coated with thin (40-300 Å) conductive metal films in order to make them suitable for STM analysis. Images such as that shown in Figure 4 possess resolution in excess of that routinely available from SEM images of these surfaces. This work demonstrated the applicability of STM to the examination of electrochemically passivated surfaces (69).

It is interesting to note that none of the STM work on metal surfaces (*i.e.*, Pt and Al) discussed above yielded images with atomic resolution. In fact, although atomic resolution images of

semi-metals such as graphite are routinely obtained in *ex situ* STM of these surfaces, the free electron nature of metals has previously been thought to be an impediment to resolving close-packed metal surfaces at atomic resolution. Notably, the close-packed surface of gold (Au(111)) has recently been imaged in both air and UHV at atomic resolution by Hallmark *et. al.* (8). This implies that atomic resolution imaging of metallic electrode surfaces may be possible in the near future. Curiously, the studies of the Au(111) surface reported an observed corrugation of 0.3 Å, which is substantially greater than that expected from theoretical calculations (70). The reasons for this discrepancy are not clear as of this date.

Adsorbate Properties. Much recent STM activity has focused on the examination of adsorbate covered surfaces. Although in several instances nonelectrochemical techniques, such as gas phase adsorption methods, have been employed to prepare these surfaces, several of these systems warrant mention here because similar adsorbates are routinely encountered in an electrochemical context.

Gimzewski *et. al.* (71) adsorbed copper phthalocyanine (CuPc) at submonolayer coverages on polycrystalline silver via sublimation *in vacuo*. These workers then imaged these surfaces in UHV with the STM. Individual copper phthalocyanine molecules were resolved at a series of tip-sample biases from 250 mV - 700 mV (tip +) at a constant current of 0.35 nA (71). At the lowest tunneling biases on this interval (narrowest tip-sample spacings), forms with disc-like geometries and diameters of ca. 10 Å were observed, as expected if CuPc were sitting flat on the surface. As the bias was increased to values > 600 mV (resulting in a greater tip-sample spacing), the shape of the observed images narrowed until a majority assumed a cone-like geometry. Significantly, stable images of individual CuPc molecules were usually observed adjacent to surface roughness. In the absence of observable roughness, stable, stationary CuPc molecules were only infrequently encountered. Instead, diffusion of CuPc molecules was observed across the STM image window at rates of ca. 2 Å/min (71). These observations demonstrate the potential for obtaining surface diffusion coefficients for adsorbed species with STM. The studies with phthalocyanines are also important from the view of electrocatalysis.

Smith *et. al.* (10) have obtained images of adsorbed sorbic acid (SA) molecules on highly ordered pyrolytic graphite substrates (HOPG) in liquid helium. Sub-monolayer coverages of sorbic acid (C_5H_7COOH) were obtained by spin-casting films from SA/benzene solutions. Images of elongated structures (Fig. 5) were associated with SA partially covering the surface. These images appeared to be composed of several SA molecules, each of which possesses dimensions 2 Å x 8 Å . At the liquid He temperatures employed for imaging in this study, gap conductivity (dI/dV) vs. tip bias spectra obtained with the STM tip positioned over SA molecules revealed peaks at energies corresponding to vibrational modes of adsorbed SA molecules as determined by IETS (72). Such spectra were typically dominated either by C=C and C-H modes, or by C=O and C-O modes, suggesting that for a given position of the STM tip over the SA molecule, tunneling current was originating primarily from the alkene end of SA molecules, or from the carboxyl moiety (10). This example is the first to demonstrate the potential of STM for extracting

spectroscopic information selectively for adsorbed molecules on a molecule by molecule basis.

In addition to the two cases discussed above, images of surfaces coated with other organic adsorbates such as cadmium arachidate Langmuir-Blodgett films, (73), DNA (74), di-methyl and di-2-ethylhexyl phthalate (75), and K-24 liquid crystals (Foster, J.S.; Frommer, J.E. Nature, submitted) have been obtained in recent publications.

Surfaces modified with polymer films (*c.f.*,76-78) and self-organizing molecular assemblies (79,80) have been of particular interest to electrochemists. Albrecht *et. al.* (Albrecht, T.R.; Dovek, M.M.; Lang, C.A.; Quate, C.F.; Kuan, W.J.; Frank, C.W.; Pease, R.F.W. J. Appl. Phys., submitted) have employed both STM and atomic force microscopy (AFM) to image, and STM to modify, poly(octadecyl acrylate) (PODA) films on HOPG. The films were prepared using Langmuir-Blodgett techniques. In this work, single PODA chains were observed on surfaces containing submonolayer coverages of the polymer. The length of the polymer chain images obtained was consistent with the known molecular weight of the PODA used in this study. Crystalline-like domains of parallel polymer bundles were also present on such surfaces. Modification of the polymer-covered surface was effected by applying a 100 nsec voltage pulse of ca. 4.1 V to the tunneling bias. In crystalline regions of the polymer coating, the application of the voltage pulse resulted in the disordering of the polymer chains and in the apparent cleaving of polymer bonds resulting in the production of shorter PODA oligomers. The mechanism for polymer bond cleavage in the STM experiment may be similar to that observed previously in electron-beam irradiation of PMMA resists.

Lithography With the STM: Nonelectrochemical Methods. The prospect of atomic density information storage has spurred applications of the STM as a surface modification tool. In this application, the anisotropic current density distribution generated by an STM tip is exploited to "write" on a substrate surface. Features with critical dimensions < 5 nm have been written in UHV, in air, and under liquids.

Although the mechanism by which modification of surfaces in UHV occurs is not clear for all cases, local heating effects appear to have effected the observed modification of glassy materials such as $Pd_{81}Si_{19}$ (81) and $Rh_{25}Zr_{75}$ (82). The fluence of electrons from an STM tip has been used to accomplish nanometer scale electron beam lithography of CaF_2 coated substrates (83). A somewhat different strategy has been employed by Silver *et. al.* (84). These workers used the electric fields of $>10^7$ V/cm present in the tunneling gap to generate a micro-plasma in the presence of an organo-metallic gas (dimethyl cadmium). The organometallic compound was reduced by the plasma, and metal deposited in 20 - 50 nm features on the cathode (substrate) surface (84). A number of recent papers (85-87) report the introduction of Angstrom scale modifications to metal surfaces by the application of large tip-sample voltages ($\Delta E_t > 2V$). Notably, these modifications have occurred both in nonpolar liquids and in air, although the mechanism by which such features are produced is not as yet clear. Finally, the STM tip itself has been

used to "micro machine" (88) surfaces by operating the STM with the tip in contact with a substrate.

Lithography With the STM: Electrochemical Techniques. The nonuniform current density distribution generated by an STM tip has also been exploited for electrochemical surface modification schemes. These applications are treated in this paper as distinct from true *in situ* STM imaging because the electrochemical modification of a substrate does not *a priori* necessitate subsequent imaging with the STM. To date, all electrochemical modification experiments in which the tip has served as the counter electrode, the STM has been operated in a two-electrode mode, with the substrate surface acting as the working electrode. The tip-sample bias is typically adjusted to drive electrochemical reactions at both the sample surface and the STM tip. Because it has as yet been impossible to maintain feedback control of the z-piezo (tip-substrate distance) in the presence of significant faradaic current (*vide infra*), all electrochemical STM modification experiments to date have been performed in the absence of such feedback control.

Lin *et. al.* (89) reported the first electrochemical modification of an electrode surface that was implemented with an STM. These workers electrochemically etched an illuminated GaAs surface with a 4 V bias (tip -) in the presence of 5 mM NaOH, 1 mM EDTA in either aqueous or acetonitrile solutions. Figure 6 shows an SEM image of a line etched on a GaAs surface using this procedure. Gas evolution at the tip cathode was prevented by adding a depolarizer such as nitrobenzene. In order to maintain a tip-substrate distance of ca. 1 μm during the etching of lines, the surface of the semiconductor was imaged with the STM in air, the resultant topographical data was stored on a computer disk, and the tip path was retraced during the etching process. Etched line widths of 2.0 μm and 0.3 μm were achieved in this seminal study (89).

Subsequent attempts at electrochemical lithography have focused principally on electrochemical metal deposition. The electrochemical deposition of metal features on the surface of a dissimilar metal is complicated by the fact that nucleation events always precede bulk metal plating (90). Thus, although the goal is generally to deposit a metal feature at a location directly under the STM tip, nucleation often occurs preferentially at surface defect sites that can be located microns away from this location (Dovek, M.M.; Heben, M.J. unpublished results, Stanford University; August, 1987). This problem is most pronounced for deposition on atomically smooth and unreactive surfaces such as basal plane-oriented HOPG, and is manifested in large nucleation overpotentials for the deposition of metals such as Ag and Cu (91). Thus, well controlled electrochemical modifications of these surfaces have not been demonstrated.

Schneir *et. al.* have avoided the nucleation problem by using the same metal (Au) for both deposition and substrate (Schneir, J.; Hansma, P.K., Elings, V.; Gurley, J.; Wickramasinghe, K.; Sonnenfeld, R. SPIE'88 Conference Proceedings, in press). These workers employed glass insulated STM tips to write 300 - 500 nm Au lines at a bias of 3.0 V and a tip-sample spacing of 1 μm. Craston *et. al.* (Craston, D.H.; Lin, C.W.; Bard, A.J. J. Electrochem. Soc.,

submitted) have achieved similar resolution by electrochemically reducing metal ions (Cu^{2+} and Ag^{+}) exchanged into Nafion-coated substrates. In this case, deposition can occur only at positions on the membrane physically contacted by the STM tip.

Clearly, the resolution attained by electrochemical methods has not yet approached that available with the other techniques discussed above. Decreasing the tip-sample distance from the 1 μm employed in previous experiments ought to localize the current density distribution and improve resolution. However, as noted above, maintaining a smaller tip-sample spacing is likely to be difficult in the absence of tunneling current feedback control. For this reason, significant improvements in electrochemical plating resolution may depend on the development of techniques for maintaining feedback controlled tunneling distances on the order of 1 - 10 nm.

In Situ STM Studies of Liquid and Solution Covered Electrode Surfaces

One of the most significant applications of STM to electrochemistry would involve the application of the full spectroscopic and imaging powers of the STM for electrode surfaces in contact with electrolytes. Such operation should enable the electrochemist to access, for the first time, a host of analytical techniques in a relatively simple and straightforward manner. It seems reasonable to expect at this time that atomic resolution images, I-V spectra, and work function maps should all be obtainable in aqueous and nonaqueous electrochemical environments. Moreover, the evolution of such information as a function of time will yield new knowledge about key electrochemical processes. The current state of STM applications to electrochemistry is discussed below.

Atomic resolution STM images of HOPG in water, and images at lower resolution of Au in aqueous 2 mM NaCl solutions, were first reported by Sonnenfeld and Hansma (57). HOPG images were obtained using total tip-sample biases of 100 mV (tip -) and total currents (faradaic + tunneling) of 50 nA. The fact that individual solvent molecules did not appear in these STM images was attributed to the fact that their high velocity relative to the tip speed resulted in time averaging (57). Itaya and Sugawara (59) subsequently reported images of HOPG in aqueous 0.05 M H_2SO_4 in the presence of residual faradaic currents of 0.2 nA (ΔE_t = 100 mV, tip -). Liu *et. al.* (92) obtained one dimensional traces with a resolution of ca. 30 nm of solution-covered, metal-coated, integrated circuits. In this case, the authors used a total current of 5 - 25 nA, which included a substantial distance-dependent faradaic current component, to control the interelectrode distance with a conventional feedback arrangement (92).

Sonnenfeld *et. al.* (58) have used STM to determine the topography of etched (0.05 v/v% Br_2/MeOH) and polished GaAs surfaces. STM images of these surfaces were obtained both in aqueous 0.01 M KOH and in concentrated aqueous NH_4OH. GaAs surfaces exposed to the chemical etchant and polished with lens paper exhibited average roughnesses of 1 nm over intervals of 5 to 1000 nm. Occasional 100 nm scale defects were also present on such surfaces. STM images of etched GaAs surfaces in 0.01 M aqueous KOH

remained unchanged over periods of several minutes (58). Interestingly, the GaAs lattice could not be resolved at these solution-covered surfaces, despite the fact that previous atomic resolution images of GaAs in UHV have been reported (3,16).

Work by Schneir, Hansma and others (86,93) has extended the list of pure liquids suitable for STM studies by demonstrating imaging capabilities with a series of nonpolar organic liquids, such as paraffin oil and fluorocarbon grease. These liquids have the advantage of possessing greater viscosity than aqueous solutions, and hence exhibit inherently smaller residual currents. These workers were able to attain tip-substrate biases (ca. 3 V) greater than those routinely possible in air or in aqueous solutions. In addition, these liquids were found to improve the signal-to-noise of the STM atomic resolution images, possibly due to improved vibrational damping characteristics as a result of the liquid layer (86,93). The authors suggest that nonpolar, organic liquids may serve to protect air sensitive or otherwise reactive surfaces, and hence facilitate the imaging of such surfaces under ambient conditions.

As noted above, Schneir, Hansma and coworkers have also used the greater biases available in nonpolar organic liquids (~ 3 V) to facilitate the surface modification of gold surfaces (87). The features introduced with this procedure were imaged *in situ* under a fluorocarbon grease. Gold mounds, initially ca. 10 nm in diameter, decreased in height and broadened over a period of 24 h as a result of diffusion. Preliminary self-diffusion coefficients for gold atoms at these surfaces of $D = 10^{-20} - 10^{-16}$ cm^2 sec^{-1} were estimated from the observed rate of change of height with time. This is the first instance in which solid-state-like diffusion coefficients have been estimated from STM images. Thus, it seems likely that room temperature diffusion coefficients might be obtained with STM for well characterized systems in the future (87).

Itaya *et. al.* (Itaya, K.; Higaki, K.; Sugawara, S. Chem. Lett., in press) have examined the nano-topography of polycrystalline Pt electrode surfaces immersed in aqueous, 0.1 M H_2SO_4 in analogy to the *ex situ* work with electrochemically activated Pt electrodes discussed above. Increases in the surface area of Pt electrodes accompanying cycling in this electrolyte are associated with electrofaceting of the electrode surface as previously reported by Baro and coworkers. The crystallographic orientation of these facets, however, is not apparent in the images reported by these authors.

Using the unique four-electrode STM described above, Bard and coworkers (Lev, O.; Fan, F-R.F.; Bard, A.J. J. Electroanal. Chem., submitted) have obtained the first images of electrode surfaces under potentiostatic control. The current-bias relationships obtained for reduced and anodically passivated nickel surfaces revealed that the exponential current-distance relationship expected for a tunneling-dominated current was not observed at the oxide-covered surfaces. On this basis, the authors concluded that the nickel oxide layer was electrically insulating, and was greater than ca. 10 Å in thickness. Because accurate potential control of the substrate surface is difficult in a conventional, two-electrode STM configuration, the ability to decouple the tip-substrate bias from

the substrate potential ought to facilitate the future study of electrode processes by STM.

Sonnenfeld and Schardt (94), and Schneir *et. al.* (Schneir, J., Hansma, P.K.; Elings, V.; Gurley, J.; Wickramasinghe, K.; Sonnenfeld, R. SPIE'88 Conference Proceedings, in press) have both reported *in situ* STM images of electrode surfaces on which metals have been electrochemically deposited. Morita *et. al.* (61) have examined Ag surfaces *in situ* in the presence of chloride ion. Figure 7 shows an STM image obtained by Sonnenfeld and Schardt (94) of a Ag island on the atomically smooth surface of HOPG in 0.05 M $AgClO_4$. This work provides insight into the mechanism by which nucleation processes occur on smooth surfaces. Because in each of the three above cases, images such as that shown in Figure 7 have been obtained in the presence of a reversible redox couple (i.e. either M^+/M^o or $AgCl/Cl^-$), they represent the most demanding conditions under which published STM images have been obtained under solution. As such, it is important to understand why STM imaging under these conditions is possible. In fact, if the correct bias polarity is selected, both of the above cases represent an example of Case I STM imaging.

The silver deposition experiments of Sonnenfeld and Schardt (94) provide a representative example. After the deposition of silver on HOPG, the freshly plated surface was imaged in the presence of aqueous 0.05 M $AgClO_4$ (Fig. 7)(94). Assuming a positive tip polarity is used, the STM tip will function as an anode and its potential will be that necessary to oxidize water, $E_{a,H2O/O2}$ = +0.95 V (pH = 7). The substrate cathode will drive the reduction of silver ion at the silver plated substrate at a formal potential of $E_{c,Ag^+/Ag}$ = +0.72 V. Thus, an imaging window of ΔE_f = 230 mV is available, inside of which neither electrochemical reaction will occur. Very different consequences result with the opposite polarity (tip -). Silver is anodically dissolved from the substrate at a reversible potential of +0.72 V, and silver ion plates at the tip cathode at the same reversible potential. Moreover, two-electrode TLC current enhancements are expected since the product at the substrate (Ag^+) is the reactant at the STM tip. In this configuration, the Ag^+/Ag system represents an example of Case II imaging, which, as noted above, is likely to be difficult with conventional, glass-coated STM tips. For this reason, Sonnenfeld and Schardt succeed in imaging Ag-plated HOPG in the presence of 50 mM Ag^+ at substantial (e.g. 100 mV) biases and positive tip polarities (94).

Thus, all of the above studies have involved Case I imaging conditions (*vide supra*). That is, in each instance, the applied biases used for imaging were less than that required to drive faradaic reactions at both tip and sample. Figure 8 shows a HOPG image obtained under 1 M NaCl at ΔE_t = 550 mV (tip +) which is representative of images achieved in 1 M NaCl at biases of $\pm$ 1.5 V and in solutions of 1 M NaCl, 0.1 M $Fe(CN)_6^{3-}$/0.1 M $Fe(CN)_6^{4-}$ solutions at biases of $\pm$ 0.8 V (Dovek, M.M.; Heben, M.J.; Lewis, N.S.; Penner, R.M.; Quate, C.F. manuscript in preparation). Since the tunneling current employed in both cases was 1 nA, we believe that these images represent the first examples of Case IV imaging. This result indicates that imaging may in fact be possible under the experimentally demanding Case IV conditions, and implies that STM

operation may be completely decoupled from electrochemical enviroments.

Summary

It should be apparent from the discussion above that STM possesses tremendous potential for the elucidation of processes at the electrode-electrolyte interface. Particularly promising are the prospects for *in situ* studies of electrode surfaces. Vibrational, electronic, and structural information is obtainable on an atomic scale for electrodes of importance to basic electrochemical studies. Although relatively few electrochemical applications have been demonstrated to date, the availability of commercial instrumentation (*c.f.*,95-97) ought to increase the accessibility of STM to electrochemists and widespread use of the technique is expected in the near future.

Acknowledgments

We acknowledge the financial assistance of the Office of Naval Research, Grant # N00014-85-K-0805. We also acknowledge the assistance of Bruce J. Tufts. NSL also acknowledges support as a Dreyfus Teacher-Scholar and as a A.P. Sloan Fellow.

Literature Cited

1. Binnig, G.; Rohrer, H.; Gerber, Ch.; Wiebel, E. App. Phys. Lett. 1982, 40, 178-80.
2. Binnig, G.; Rohrer, H.; Gerber, Ch.; Weibel, E. Phys. Rev. Lett., 1982, 49, 57-61.
3. Feenstra, R.M.; Stroscio, J.A.; Tersoff, J.; Fein, A.P. Phys.Rev. Lett. 1987, 58, 1192-95.
4. Jaklevic, R.C.; Elie, L. Phys. Rev. Lett. 1988, 60, 120-23.
5. Becker, R.S.; Golovchenko, J.A.; Swartzentruber, B.S. Phys.Rev. Lett. 1985, 54, 2678-80.
6. Binnig, G.; Rohrer, H.; Gerber, Ch.; Weibel, E. Phys.Rev. Lett. 1983, 50, 120-23.
7. Hamers, R.J.; Avouris, Ph.; Bozso, F. Phys. Rev. Lett. 1987, 59, 2071-74.
8. Hallmark, V.M.; Chiang, S.; Rabolt, J.F.; Swalen,J.D.; Wilson, R.J. Phys. Rev. Lett. 1987, 59, 2879-82.
9. Slough, C.G.; McNairy, W.W.; Coleman, R.V.; Drake, B.; Hansma, P.K. Phys. Rev. B 1986 34, 994-1005.
10. Smith, D.P.E.; Kirk, M.D.; Quate, C.F. J. Chem. Phys. 1987, 86, 6034-38.
11. Miranda, R.; Garcia, N.; Baro, A.M.; Garcia, R.; Pena, J.L.; Rohrer, H., Appl. Phys. Lett. 1985, 47,367-69.
12. Park, S.; Quate, C.F. Appl. Phys. Lett. 1986 48, 112-14.
13. Abraham, D.W.; Sattler, K.; Ganz, E.; Mamin, H.J.;Thomson, R.E.; Clarke, J. Appl. Phys. Lett. 1986, 49, 853-55.
14. Carim, A.H.; Dovek, M.M.; Quate, C.F.; Sinclair, R.;Vorst, C. Science 1987, 237, 630-33.
15. Kaiser, W.J.; Jaklevic, R.C. IBM J. Res. Develop. 1986, 30, 411-16.

16. Stroscio, J.A.; Feenstra, R.M.; Fein, A.P. Phys. Rev. Lett. 1987 58, 1668-71.
17. Hamers, R.J.; Tromp, R.M.; Demuth, J.E. Phys. Rev.Lett. 1986, 56, 1972-75.
18. Binnig, G.; Fuchs, H.; Gerber, Ch.; Rohrer, H.; Stoll, E.; Tosatti, E. Europhys. Lett. 1986 31, 1-36.
19. Quate, C.F. Phys. Today 1986, August, 26-33.
20. Hansma, P.K; Tersoff, J. J. Appl. Phys. 1987, 61, R1-R23.
21. Binnig, G.; Rohrer, H. Sci. Am. 1985, August, 50-56.
22. Feuchtwang, T.E.; Cutler, P.H. Phys. Scr. 1986, 35,132-40.
23. Arvia, A.J. Surf. Sci. 1987 181, 78-91.
24. Fleischmann, M.; Hendra, P.J.; McQuillan, P.J. Chem. Phys. 1964 26, 163-67.
25. Jeanmaire, D.L.; Van Duyne, R.P. J. Electroanal.Chem. 1974, 84, 1-20.
26. Albrecht, M.G.; Creighton, J.A. J. Am. Chem. Soc. 1977, 99, 5215-17.
27. Tersoff, J.; Hamann, D.R. Phys. Rev. B 1985, 31, 805-13.
28. Lang, N.D. Phys. Rev. Lett. 1986, 56, 1164-67.
29. Binnig, G.; Rohrer, H. Surf. Sci. 1983, 126, 236-44.
30. Bryant, A.; Smith, D.P.E.; Quate, C.F. Appl. Phys. Lett. 1986, 48, 832-34.
31. Chiang, S.; Wilson, R.J. Anal. Chem. 1987, 59, 1267A-70A.
32. Binnig, G.; Rohrer, H. Physica B&C 1984 127B,37-45.
33. Binnig, G.; Gerber, Ch.; Stoll, E.; Albrecht, T.R.; Quate, C.F. Europhys. Lett. 1987 3, 1281-86.
34. Heinzelmann, H.; Grutter, P.; Meyer, E.; Hidber, H.; Rosenthaler, L.;Ringger, M.; Guntherodt, H.-J., Surf. Sci. 1987 189/190, 29-35.
35. Albrecht, T.R.; Quate, C.F. J. Appl. Phys. 1987, 62, 2599-602.
36. Heinz, K.; Muller, K. In Structural Studies of Solids Springer Tracts in Modern Physics: New York, 1982; vol. 91, pp 1-17.
37. Broers, A.N. Rev. Sci. Instr. 1969 40, 1040-45.
38. Allen, F.M.; Smith, B.K.; Buseck, P.R. Science 1987 238, 1695-97.
39. Blum, L.; Abruna, H.D.; White, J.; Gordon II, J.G.; Borges, G.L.; Samant, M.G.; Melroy, O.R. J. Chem. Phys. 1986, 85, 732-38.
40. Samant, M.G.; Borges, G.L.; Gordon II, J.G.; Melroy, O.R.; Blum, L.; J. Am. Chem. Soc. 1987, 109, 5970-74.
41. Materlik, G.; Schmah, M.; Zegenhagen, J.; Uelhoff, W. Ber. Bunsenges. J. Phys. Chem. 1987, 91, 292-96.
42. Kruger, J. In Advances in Electrochemistry and Electrochemical Engineering; Muller, R.H., Ed.; Wiley and Sons: New York, 1973; vol. 9, pp 227-280.
43. Muller, R.H. In Advances in Electrochemistry and Electrochemical Engineering; Muller, R.H., Ed.; Wiley and Sons: New York, 1973; vol. 9, pp 167-226.
44. Lehwald, S. and Ibach, H. In Vibrations at Surfaces; Caudano, R., Gilles, J.-M. and Lucus, A.A. Eds.; Plenum Press: New York, 1982; pp 137-152.
45. Wolf, E.L. Principles of Electron Tunneling Spectroscopy; Oxford University Press: New York, 1985, Chapter 10.
46. Pons, S., Davidson, T.; Bewick, A. J. Electroanal. Chem. 1984, 160, 63-71.

47. Birke, R.L., Lombardi, J.R., and Sanchez, L.A. In Electrochemical and Spectroscopic Studies of Biological Redox Components; Kadish, K. Ed.; ACS Symposium Series No.210; American Chemical Society: Washington, DC, 1981; p 69.
48. Feenstra, R.M.; Stroscio, J.A.; Fein, A.P. Surf. Sci. 1987, 181, 295-306.
49. Demuth, J.; Avouris, P. Phys. Today 1983, November, p 62.
50. Reihl, B.; Gimzewski, J.K. Surf. Sci. 1987, 189/190, 36-43.
51. Bryant, A. Ph.D. dissertation, Stanford University, June, 1986.
52. Binnig, G.; Gerber, C.; Marti, O. IBM Tech. Discl. Bull. 1984 27, 3137.
53. Gerber, Ch.; Binnig, G.; Fuchs, H.; Marti, O.; Rohrer, H. Rev. Sci. Instr. 1986 57, 221-24.
54. Bryant, A.; Smith, D.P.E.; Quate, C.F. Appl. Phys. Lett. 1986 48, 832-834.
55. Pohl, D.W. IBM J. Res. Develop. 1986, 30, 417-27.
56. Binnig, G.; Smith, D.P.E. Rev. Sci. Instru. 1986 57, 1688-89.
57. Sonnenfeld, R.; Hansma, P.K. Science 1986 232, 211-13.
58. Sonnenfeld, R.; Schneir, J.; Drake, B.; Hansma, P.K.; Aspnes, D.E. Appl. Phys. Lett. 1987 50, 1742-44.
59. Itaya, K.; Sugawara, S. Chem. Lett. 1987, 1927-30.
60. Morita, S.; Okada, T.; Ishigame, Y.; Mikoshiba, N. Surf. Sci. 1987 181, 119-25.
61. Morita, S.; Otsuka, I.; Okada, T.; Yokoyama, H.; Iwasaki, T.; Mikoshiba, N. Jap. J. Appl. Phys. 1987 26, L1853-55.
62. Bard, A.J.; Faulkner, L.R. Electrochemical Methods: Fundamentals and Applications; John Wiley & Sons: New York, 1980, p 699.
63. Hubbard, A.T.; Anson, F.C. In Electroanalytical Chemistry; Bard, A.J., Ed.; Marcel Dekker: New York, 1970; vol. 4, p 129.
64. Davis, J.M.; Fan, F-R.F.; Bard, A.J. J. Electroanal. Chem. 1988, 238, 9-31.
65. Wightman, R.M. Anal. Chem. 1981, 53, 1126A-31A.
66. Geng, L.; Reed, R.A.; Longmire, M.; Murray, R.W. J. Phys. Chem. 1987, 91, 2908-14.
67. Gomez, J.; Vasquez, L.; Baro, A.M.; Garcia, N.; Perdriel, C.L.; Triaca, W.E.; Avria, A.J. Nature 1986 323, 612-14.
68. Vasquez, L.; Gomez, J.; Baro, A.M.; Barcia, N.; Marcos, M.L.; Velasco, J.G.; Vara, J.M.; Arvia, A.J.; Presa, J.; Garcia, A.; Aguilar, M. J. Am. Chem. Soc. 1987, 109, 1730-33.
69. Morita, S.; Itaya, K.; Mikoshiba, N. Jap. J. Appl. Phys. 1986 25, L743-45.
70. Batra, I.P.; Barker, J.A.; Auerbach, D.J. J. Vac. Sci. Technol. A 1984, 2, 943-47.
71. Gimzewshi, J.K.; Stoll, E.; Schlittler, R.R. Surf. Sci. 1987, 181, 267-77.
72. Hall, J.T.; Hansma, P.K. Surf. Sci. 1978, 76, 61-76.
73. Smith, D.P.E.; Bryant, A.; Quate, C.F.; Rabe, J.P.; Gerber, Ch.; Swalen, J.D. Proc. Natl. Acad. Sci. USA 1987, 84, 969-72.
74. Binnig, G. Bull. Am. Phys. Soc. 1986, 31, 217.
75. Foster, J.S.; Frommer, J.E.; Arnett, P.C. Nature 331, 324-26.
76. Wrighton, M.S. Science 1986, 231, 32-37.
77. Murray, R.W. Acc. Chem. Res. 1980, 13, 135-41.
78. Buttry, D.A.; Anson, F.C. J. Am. Chem. Soc. 1983, 105, 685-89.
79. Miller, C.J.; Majda, M. J. Am. Chem. Soc. 1986, 108, 3118-20.

80. Finklea, H.O.; Robinson, L.R.; Blackburn, A.; Richter, B.; Allara, D.; Bright, T. Langmuir 1986, 2, 239-44.
81. Ringger, M.; Hidber, H.R.; Schlog, R.; Oelhafen, P.; Guntherodt, H.J. Appl. Phys. Lett. 1985, 46, 832-34.
82. Staufer, U.; Wiesendanger, R.; Eng, L.; Rosenthaler, L.; Hidber, J.R.; Guntherodt, H.-J. Appl. Phys. Lett. 1987, 51, 244-46.
83. McCord, M.A.; Pease, R.F.W. J. Vac. Sci. Technol. B 1987, 5, 430-33.
84. Silver, R.M.; Ehrichs, E.E.; de Lozanne, A.L. Appl. Phys. Lett. 1987, 51, 247-49.
85. Becker, R.S.; Golovchanko, J.A.; Swartzentruber, B.S. Nature 1987, 325, 419-21.
86. Schneir, J.; Hansma, P.K. Langmuir 1987, 3, 1025-27.
87. Schneir, J.; Sonnenfeld, R.; Marti, O.; Hansma, P.K.; Demuth, J.E.; Hamers, R.J. J. Appl. Phys. 1988, 63, 717-21.
88. McCord, M.A.; Pease, R.F.W. Appl. Phys. Lett. 1987, 50, 569-70.
89. Lin, C.W.; Fan, F-R.F.; Bard, A.J. J. Electrochem. Soc. 1987, 134, 1038-39.
90. Kolb, D.M. In Advances in Electrochemistry and Electrochemical Engineering; Gerischer, H. and Tobias,C.W., Eds.; John Wiley & Sons: New York, 1978; vol. 2, p 125.
91. Morcos, I. J. Electroanal. Chem. 1975, 66, 250-57.
92. Liu, H-Y.; Fan, F-R.F.; Lin, C.W.; Bard, A.J. J. Am. Chem. Soc. 1986, 108, 3838-39.
93. Giambattista, B.; McNairy, W.W.; Slough, C.G.; Johnson, A.; Bell, L.D.; Coleman, R.V.; Schneir, J.; Sonnenfeld, R.; Drake, B.; Hansma, P.K. Proc. Nat. Acad. Sci. USA 1987, 84, 4671-74.
94. Sonnenfeld, R.; Schardt, B.C. Appl. Phys. Lett. 1986, 49, 1172-74.
95. Nanoscope, Digital Instruments, Inc., 5901 Encina Rd., Goleta, CA 93117.
96. WA Technology Inc., 41 Accord Park Drive, Norwell, MA 02061.
97. McAllister Technical Services, Inc., 2414 Sixth Street, Berkeley, CA 94710.

Figure 1. Single tube piezo, solution STM of Sonnenfeld and Hansma with fluid transfer line. Reproduced with permission of Ref. 58. Copyright 1986 American Institute of Physics.

Figure 2. Solution STM design with single tube piezo, remote approach and fast retract capabilities, large solution capacity, and solution-insulated tip (tip design inset) (Dovek, M.M.; Heben, M.J.; Lang, C.; Lewis, N.S.; Quate, C.F. Rev. Sci. Instr., submitted).

Figure 3. $i_{F,TLC}/i_{F,hsph}$ vs. γ for conical-planar two electrode cell (A) and hemispherical-planar two electrode cell (B). Calculated using Eqs. 2 and 3 (64).

Figure 4. STM images of Al_2O_3 barrier oxide formed anodically at an applied potential of 20 V in Aq. 20 w/v% H_2SO_4. Surface was coated with 300 Å of Pt-Pd alloy prior to imaging. The image at left is a composite of the six STM images at right which were obtained with y-piezo offset voltages as shown. Reproduced with permission of Ref. 69. Copyright 1986 Japanese Journal of Applied Physics.

Figure 5. Sorbic acid molecules on HOPG as reported by Smith *et. al.* (10). This surface was prepared by spin-coating a dilute sorbic acid-benzene solution onto a freshly cleaved HOPG substrate. Images of the surface were obtained in liquid helium. The elongated structure shown was representative of those present on surfaces prepared with this procedure. Reproduced with permission of Ref. 10.

Figure 6. Scanning electron micrograph (SEM) of n-GaAs surface electrochemically etched with a scanning electrochemical and tunneling microscope (SETM). Etching was accomplished in Aq. 5 mM NaOH, 1 mM EDTA. Photoelectric current = 0.7 mA, Scan rate = 0.1 mm/sec, bias voltage = 4 V. Tip was moved in an "L" pattern. Reproduced with permission of Ref. 89. Copyright 1987 The Electrochemical Society Inc.

Figure 7. STM images of a silver island on HOPG in aqueous 0.05 M $AgClO_4$. Image was obtained with a glass-coated Pt-Ir tip at a bias of 100 mV (tip +) and i_t = 16 nA without removing the freshly Ag plated surface from the plating solution. Reproduced with permission of Ref. 94. Copyright 1986 American Institute of Physics.

Figure 8. STM image of the basal-plane surface of HOPG obtained in 1 M NaCl. Bias = 550 mV (tip +), i_t = 1 nA. Image was obtained in the fast scan mode. Carbon atoms (dark spots) are separated from each other by 2.5 A.

Figure 1

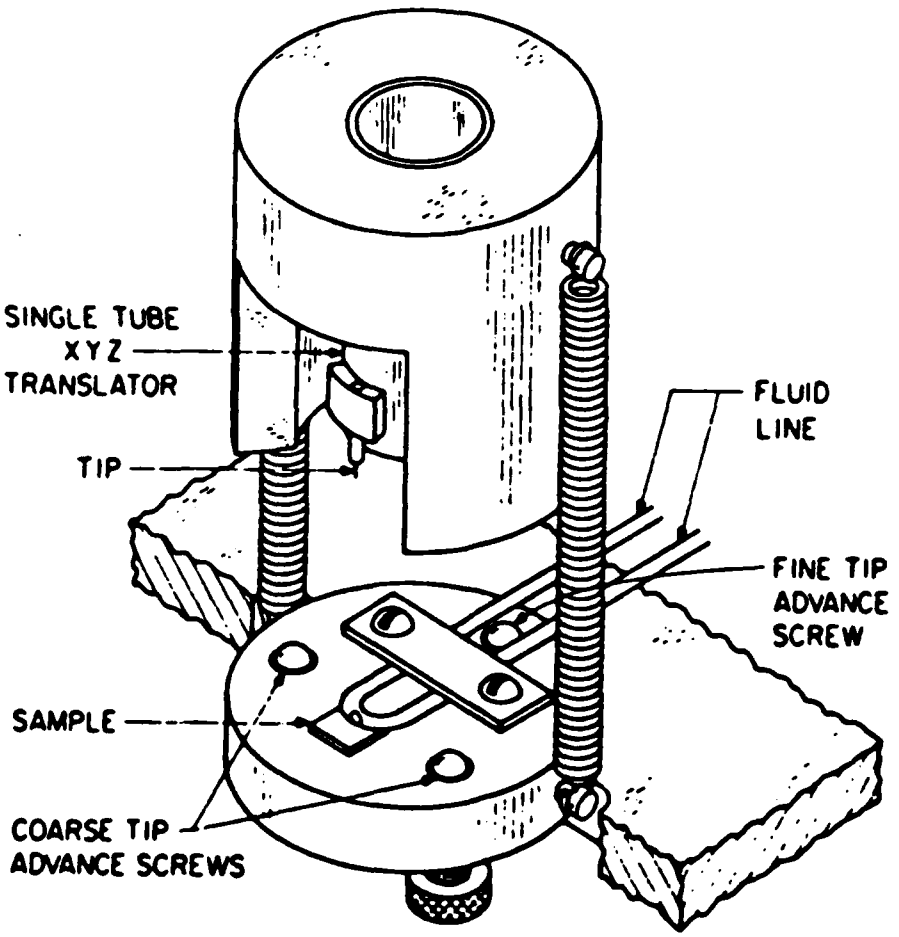
SINGLE TUBE
XYZ
TRANSLATOR
TIP
FLUID
LINE
FINE TIP
ADVANCE
SCREW
SAMPLE
COARSE TIP
ADVANCE SCREWS

Figure 2

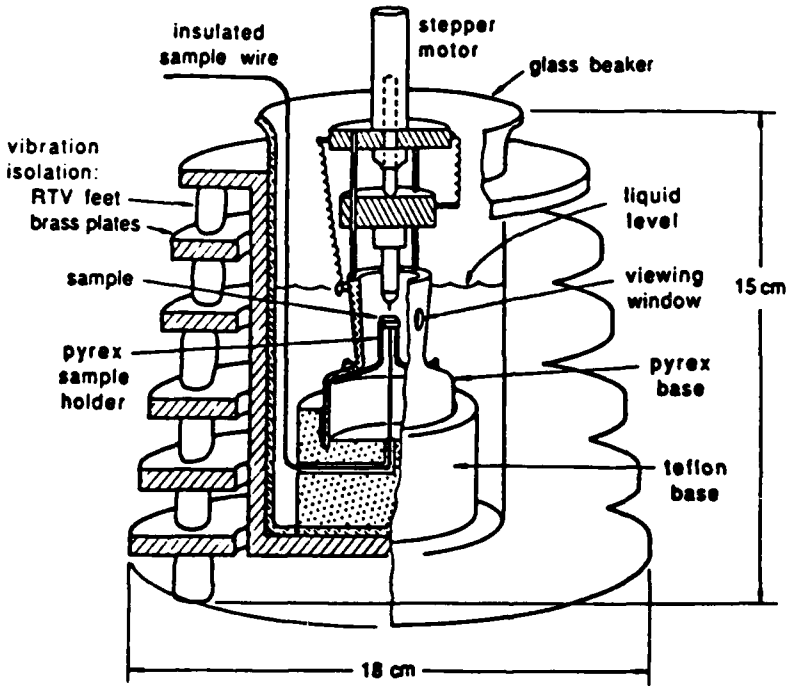
insulated
sample wire
stepper
motor
glass beaker
vibration
isolation:
RTV feet
brass plates
liquid
level
sample
viewing
window
15 cm
pyrex
sample
holder
pyrex
base
teflon
base
18 cm

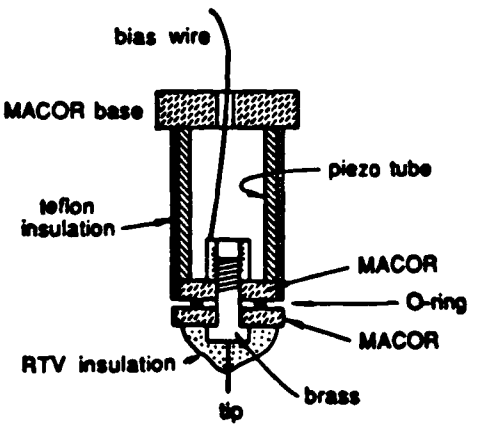
bias wire
MACOR base
piezo tube
teflon
insulation
MACOR
O-ring
MACOR
RTV insulation
brass
tip

Figure 3

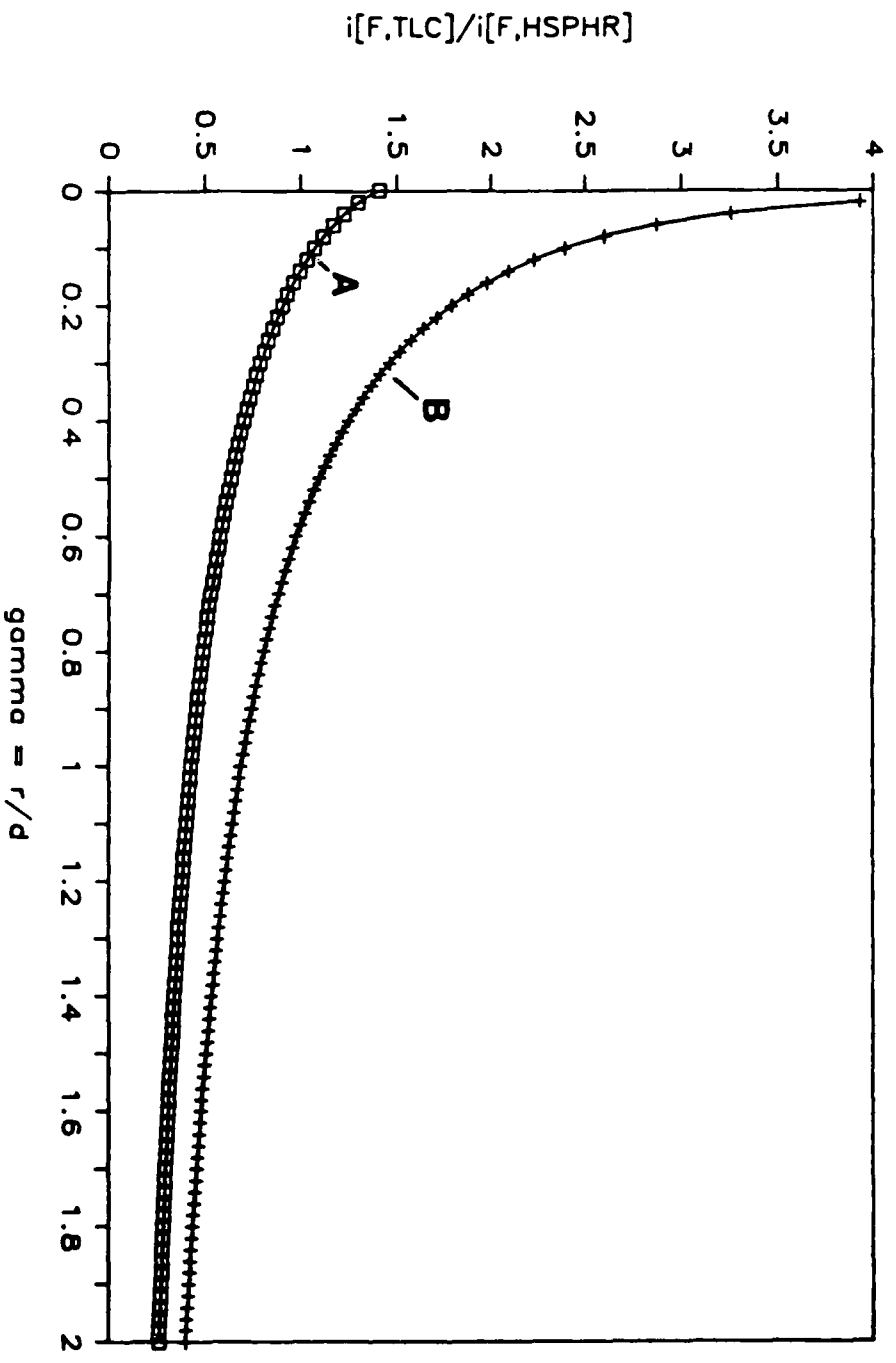
i[F,TLC]/i[F,HSPHR]
0
0.5
1
1.5
2
2.5
3
3.5
4
0
0.2
0.4
0.6
0.8
1
1.2
1.4
1.6
1.8
2
gamma = r/d
A
B

Figure 4

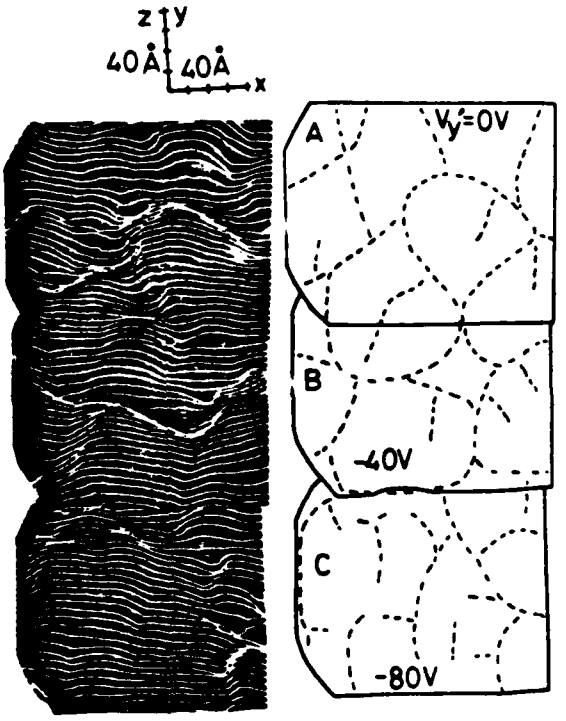

Figure 5

Figure 6

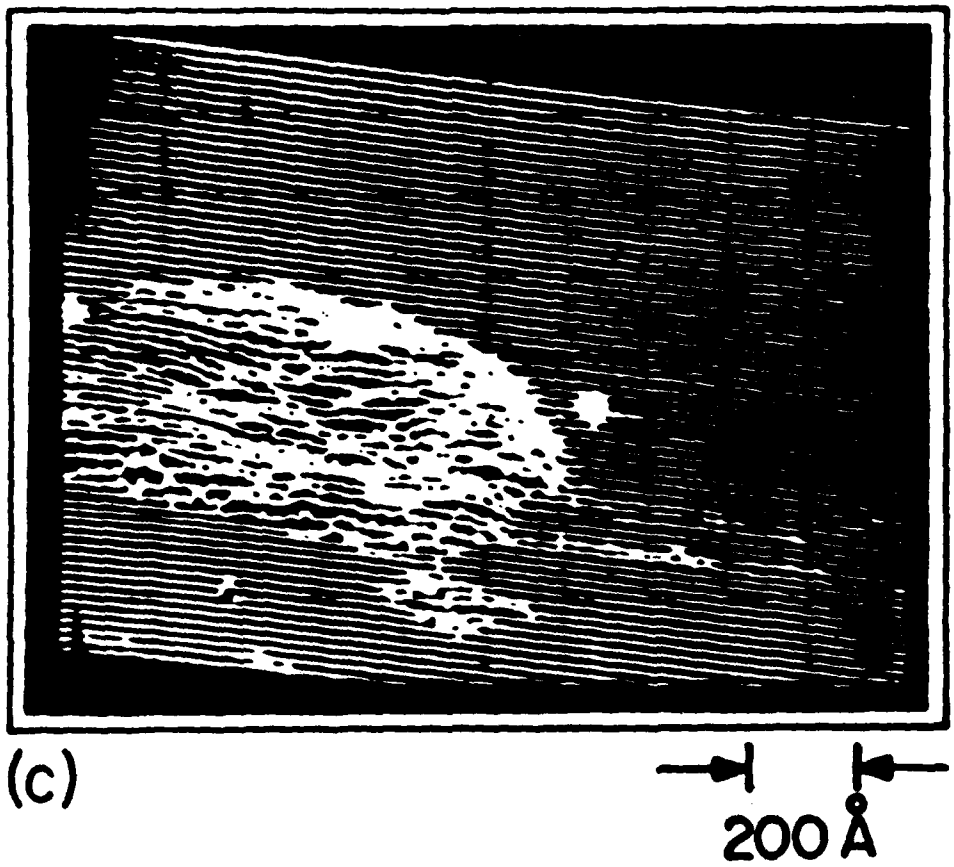

Figure 7

Fig 8